Available online at www.sciencedirect.com

SCIENCE DIRECT

Biochimica et Biophysica Acta 1664 (2004) 257–266

BIOCHIMICA ET BIOPHYSICA ACTA
BBA
www.bba-direct.com

Phospholipid membrane bending as assessed by the shape sequence of giant oblate phospholipid vesicles

J. Majhenc[a,*], B. Božič[a], S. Svetina[a,b], B. Žekš[a,b]

[a] *Institute of Biophysics, Faculty of Medicine, University of Ljubljana, Lipičeva 2, SI-1000 Ljubljana, Slovenia*
[b] *Jožef Stefan Institute, Jamova 39, SI-1000 Ljubljana, Slovenia*

Received 8 December 2003; received in revised form 8 June 2004; accepted 15 June 2004
Available online 4 July 2004

Abstract

Vesicle shape transformations caused by decreasing the difference between the equilibrium areas of membrane monolayers were studied on phospholipid vesicles with small volume to membrane area ratios. Slow transformations of the vesicle shape were induced by lowering of the concentration of lipid monomers in the solution outside the vesicle. The complete sequence of shapes consisted of a string of pearls, and wormlike, starfish, discocyte and stomatocyte shapes. The transformation from discocyte to stomatocyte vesicle shapes was analyzed theoretically to see whether these observations accord with the area difference elasticity (ADE) model. The membrane shape equation and boundary conditions were derived for axisymmetrical shapes for low volume vesicles, part of whose membranes are in contact. Calculated shapes were arranged into a phase diagram. The theory predicts that the transition between discocyte and stomatocyte shapes is discontinuous for relatively high volumes and continuous for low volumes. The calculated shape sequences matched well with the observed ones. By assuming a linear decrease of the equilibrium area difference with time, the ratio between the nonlocal and local bending constants is in agreement with reported values.

Keywords: Phospholipid vesicle; Membrane; Area difference elasticity model

1. Introduction

Phospholipid molecules in an aqueous environment tend to aggregate into bilayers. When a bilayer closes upon itself, it forms a phospholipid vesicle which may exhibit a large variety of shapes [1–3]. The shape of a vesicle with a certain membrane area depends on its volume, on the number of molecules in each of the bilayer leaflets and on the membrane elasticity. An appropriate model for the elastic properties of phospholipid membranes is the area difference elasticity (ADE) model [4–6].

According to the ADE model, the elastic properties of a vesicle membrane can be described by the area expansivity elastic constant (K), and the local (k_c) and the nonlocal (k_r) bending constants. These elastic constants reflect the ability of the membrane to stretch, to bend and to expand one monolayer relative to the other. Different methods have been used for their determination. Rawicz et al. [7] measured the area expansivity elastic constant and the local bending constant for several phosphatidylcholine membranes by aspiration of a vesicle into a micropipette. The obtained values were $K = 0.24$ N/m and k_c between 0.4×10^{-19} and 1.2×10^{-19} J, depending on chain length and saturation of the lipids. The local bending constant has also been determined by measurements of thermal fluctuations of nearly spherical vesicles [8–10] and of long tubular vesicles [11,12]. The values of k_c for different phospholipid membranes lie between 0.5×10^{-19} and 1.5×10^{-19} J [10]. The nonlocal and local bending constants have been determined simultaneously by a tether pulling method, where a thin membrane cylinder (tether) is pulled out of an aspirated vesicle [13–15]. The value for the nonlocal bending constant for L-α-stearoyl-oleoyl-glycero-phosphocholine (SOPC) membrane is estimated to be two to three times larger than the local bending constant.

An alternative method for assessing the elastic properties of phospholipid membranes is based on the observation of shapes of freely buoyant vesicles [16,17]. By observing

* Corresponding author. Tel: +386-1-543-7600; fax: +386-1-431-51-27.
E-mail address: janja.majhenc@biofiz.mf.uni-lj.si (J. Majhenc).

0005-2736/$ - see front matter © 2004 Elsevier B.V. All rights reserved.
doi:10.1016/j.bbamem.2004.06.006

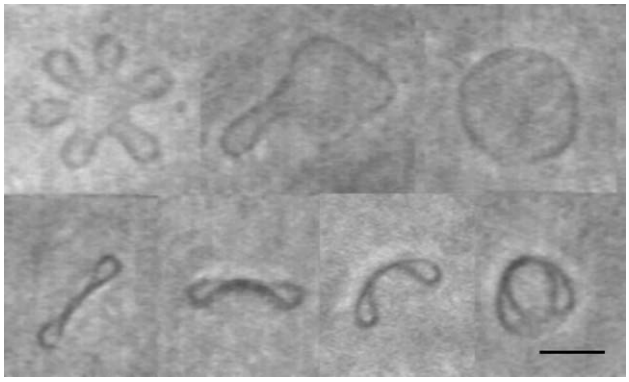

Fig. 1. An example of the observed transformation of a vesicle. The starfish vesicle was selected in the sample and the shape transformations were followed. The third and the fourth pictures are the two projections of the discocyte shape. The bar indicates 10 μm.

spinodal shape transitions of nearly spherical vesicles and applying the ADE model, it is possible to extract information about the ratio between the nonlocal and local elastic constants of membranes. Döbereiner et al. [16] obtained a value of 3 for the ratio between nonlocal and local bending constants for SOPC vesicles. In this paper we extend their approach by studying the shape transformations of vesicles with smaller ratio between the volume and membrane area than theirs. In such vesicles the shape changes are more pronounced and the corresponding elastic energies are larger which may enhance the sensitivity of the method in assessing the vesicle elastic properties. The shape transformations are induced by lowering the concentration of monomeric lipid in the surrounding solution. The observed shape transformations of vesicles correspond to a decreasing difference between the equilibrium areas of monolayers. Shape transformations of the vesicles, without changing the membrane composition, were induced previously by increasing the temperature [2] and by applying optical tweezers [18].

The approach applied here is based on the comparison of the vesicle shapes recorded by phase contrast microscopy and the theoretical predictions based on the ADE model [4,6]. Within this model we can determine the axisymmetrical shapes of discocyte and stomatocyte vesicles and arrange them into the corresponding phase diagram. Similar shapes have been analyzed theoretically for the flaccid vesicles [6,19,20], but not for vesicles with small volumes to membrane area ratios, which may have some parts of their membranes in contact (Fig. 1). Special attention will be devoted to the exact determination of such shapes.

2. Methods and analysis

2.1. Preparation and observation of vesicles

SOPC was obtained as a powder from Avanti Polar Lipids (Alabama, USA), and used without further purification. The purity of the lipid indicated by the producer was better than 99%. It was dissolved in a mixture of the chloroform and methanol (1:1 v/v) at 1 mg/ml and stored at −10 °C. Giant vesicles were prepared by a modified method of Reeves and Dowben [21]. Approximately 40 μl of lipid solution was spread on a Teflon disk and left for at least 2 h under low vacuum for the solvent to evaporate. The Teflon disk with lipid film was placed at the bottom of 50-ml glass beaker, and 10-ml glucose solution (0.2 mol/l) was added. The system was left to stand for some hours at room temperature. Vesicles grew spontaneously, as indicated by the appearance of a white foggy cloud above the Teflon disc. The stock suspension of the vesicles was kept in the same glass beaker and used for measurements during the next few days.

Just before the observation, a small volume of stock suspension was taken from the beaker and mixed with the same volume of isomolar glucose solution (1:1 v/v), in order to dilute the molecular phosholipids in the solution to below the critical vesicle concentration (CVC) [22]. This mixture was then placed in the observation chamber.

The observation chamber consisted of two glass plates separated by a layer of vacuum grease. Evaporation from the chamber was prevented, to keep the glucose concentration of the surrounding solution constant and thus to keep the vesicle volume constant during the observation. Vesicles were observed under a microscope (Zeiss IM35) with phase contrast objective (Zeiss 100 X Ph3, NA = 1.3). The microscope was equipped with a black and white CCD-camera (Sony SSC-M370CE) with 752 × 582 pixels and a video recorder (Sony U-Matic, VO 9800P). The pictures were digitized on an 8-bit frame grabber (DT 2851, Data Translation Inc.) and analyzed with a homemade image analysis software.

The measurements were made on giant unilamellar (membrane composed of a single bilayer) vesicles with small volume to membrane area ratios. For each observation, a vesicle with small volume to membrane area ratio was selected from the vesicles in the suspension and monitored. The complete sequence of vesicle shapes was observed to be: a string of pearls, wormlike shapes, either straight or branched, starfish shapes, oblate discocyte shapes and stomatocyte shapes. The neck of the stomatocyte gradually narrowed and finally closed. When the neck closed, the shape of the vesicle attained a limiting shape that is composed of a sphere with an invaginated smaller sphere. In some vesicles the observations were started with starfish or discocyte shapes (Fig. 1). The reverse order of the described or similar vesicle shape sequence was never observed. Because it took some time to find an appropriate vesicle in the solution, the observation of the shape changes started usually 2–15 min after the sample preparation. If such a vesicle was not found in half an hour, the sample was discarded. Although most low volume vesicles showed shape transformations, only a small proportion of them had volume to membrane area ratio appropriate for analysis

and remained axisymmetrical through the sequence of shape transformations.

We restricted our analysis to the shape transitions from the discocyte shape to the described limiting shape.

2.2. Membrane elastic energy and the determination of vesicle shapes

In general, the shapes of flaccid vesicles are governed by the elastic energy of the vesicle membrane (W_{el}). According to the ADE model, in the case of non-extensible membrane ($K=\infty$), the elastic energy of the membrane, composed of two elastic monolayers, is the sum of the local (W_b) and the nonlocal (W_r) bending terms [4,6,23] and can be expressed by

$$W_{el} = W_b + W_r = \frac{k_c}{2}\int (c_1 + c_2 - c_0)^2 dA + \frac{k_r}{2Ah^2}(\Delta A - \Delta A_0)^2, \quad (1)$$

where k_c and k_r are the bending and the nonlocal bending constants, c_1 and c_2 are the principal curvatures, c_0 is the spontaneous curvature of the membrane, A is the membrane area, h is the distance between the neutral surfaces of the outer and the inner monolayers, ΔA is the difference between the areas of the neutral surfaces of the two monolayers, and ΔA_0 is the corresponding equilibrium area difference. The difference between the areas of the monolayers is given by the integral $\Delta A = h\int(c_1 + c_2)dA$, and thus depends on the vesicle shape, whereas the difference between the equilibrium areas of the two layers (ΔA_0) is determined by the number of lipid molecules composing the layers and by the area of a phospholipid molecule at equilibrium. The nonlocal bending term represents the energy required to change the relative packing of molecules in the two monolayers of the bilayer.

It is convenient to present the theoretical results in reduced units, relative to the values of a sphere with vesicle membrane area (A). The dimensions of the vesicle are thus given relative to the radius of this sphere ($R_0=(A/4\pi)^{1/2}$). The relevant parameters determining the equilibrium shape are the reduced volume of the vesicle ($v = 3V/4\pi R_0^3$) and the reduced difference between the equilibrium areas of the membrane monolayers ($\Delta a_0 = \Delta A_0/(8\pi h R_0)$). The reduced difference between the areas of the membrane monolayers is $\Delta a = \Delta A/(8\pi h R_0)$. The spontaneous curvature (c_0) is taken to be zero, because the membrane is symmetrical and the solutions inside and outside of the vesicle are the same.

The equilibrium vesicle shape corresponds to the minimum of the elastic energy (Eq. (1)) at given values of the parameters v and Δa_0. This shape can be obtained by solving the corresponding variational problem. The derivation of the resulting differential equation for the axisymmetrical shape is shown in Appendix A. Special attention is devoted to shapes with small reduced volumes, where parts of the membrane are in contact. The symmetric and asymmetric shapes with respect to the vesicle equatorial plane are in this case called torocytes and codocytes, respectively [24]. For torocytes and codocytes, we distinguish two sections. The section where two parts of the membrane are in contact can be considered as a double bilayer. On both sides of the double bilayer there is the same surrounding solution at the same pressure. Both parts of the double bilayer belong to the same membrane that is uniformly strained, and thus exhibits the same lateral tension and the same difference between the lateral tensions of monolayers (relative tension). In the double bilayer the difference between the lateral tensions of monolayers in one bilayer compensates the same difference in the second bilayer, which makes the relative tension of this section to be effectively zero. It is assumed that the interactions between the bilayers in the double bilayer are negligible. When calculating the shapes of the oblate vesicles of small reduced volume, we have to take into consideration that there are neither external forces nor external torques acting at the rim of the double bilayer section.

For any given values of v, Δa_0 and the ratio k_r/k_c, the equilibrium shape of a vesicle and the corresponding value of Δa can be calculated. Thus, for given values of the reduced volume and the ratio k_r/k_c, the interrelation between Δa and Δa_0 can be deduced. The theoretical results are presented for a ratio between the elastic constants (k_r/k_c) of 3. The shapes of axisymmetric oblate vesicles were calculated as a function of the reduced volume (v) and the reduced difference between the equilibrium areas of the outer and the inner monolayers (Δa_0) and arranged into a phase diagram. The phase diagram is divided into five shape regions: discocyte, stomatocyte, codocyte, torocyte, and a larger sphere with an invaginated smaller sphere. Point C in Fig. 2 is a critical point at which the character of the shape transition changes with respect to the equatorial mirror symmetry. Namely, for the chosen ratio $k_r/k_c = 3$, it is predicted that the vesicles with a reduced volume smaller than 0.58 exhibit continuous shape transformation between the discocyte and stomatocyte shapes, and that vesicles with reduced volumes larger than 0.58 exhibit a discontinuous shape transformation. The discontinuous shape transformation is more pronounced at larger deviations of the reduced volume from the critical value (0.58). For higher ratios k_r/k_c, the critical point C moves to larger reduced volumes.

In order to visualize two qualitatively different transitions between the discocyte and stomatocyte shapes, the dependence of the shapes and reduced area difference (Δa) on the reduced equilibrium area difference (Δa_0) is presented in Fig. 3 for two different reduced volumes. At reduced volume $v = 0.3$, the shape changes are continuous. The discontinuous transition between discocytic and stomatocytic shapes at the large reduced volume (0.7) can be noted as the jump in Δa, which is indicated by the dashed line.

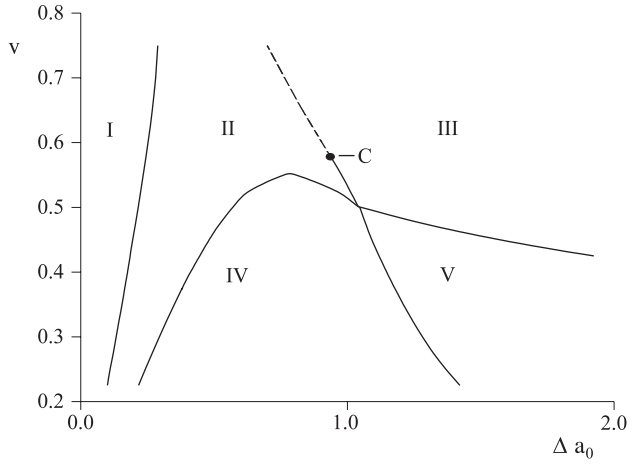

Fig. 2. The phase diagram for axisymmetric oblate vesicles at $k_r/k_c = 3$ as a function of the reduced volume (v) and the reduced equilibrium difference between the areas of the outer and the inner monolayers (Δa_0). The region of the limiting shapes, i.e., two spheres connected by an infinitesimally narrow neck, is indicated by I, of stomatocytic shapes II, discocytic shapes III, codocytic shapes IV, and torocytic shapes V. C is the critical point at which the character of the shape transition with respect to equatorial mirror symmetry changes. At lower volumes there is a continuous transition between discocytes and stomatocytes, indicated by the solid line, and at larger volumes there is a discontinuous transition, indicated by the dashed line.

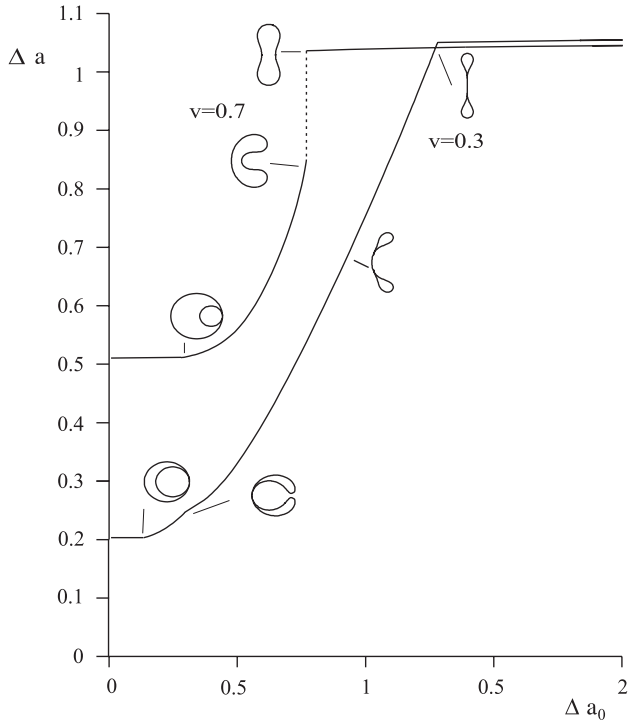

Fig. 3. The dependence of the reduced difference between the areas of membrane monolayers (Δa) on the reduced equilibrium difference between the areas of the membrane monolayers (Δa_0) for the reduced volumes (v) 0.7 and 0.3, and the ratio between the local and nonlocal bending constants $k_r/k_c = 3$. The dashed line shows the position of the discontinuous transition between the discocyte and stomatocyte shapes for the reduced volume 0.7. In order to visualize the shape changes, some characteristic shapes are presented.

2.3. The analysis of the experiments

The analysis is focused on the shape transitions in the range of shapes from discocytes to stomatocytes with a closed neck (cf. Fig. 1). Theoretically the shapes in this range are axisymmetrical and depend solely on the reduced volume (v) and the reduced difference between the areas of the membrane monolayers (Δa). The reduced volume of a given vesicle is constant during the observation. It can be determined from the radii of the outer (R_{Li}) and the inner (R_{Lo}) spheres of the limiting shape (Fig. 4a),

$$v_L = \frac{R_{Lo}^3 - R_{Li}^3}{(R_{Lo}^2 + R_{Li}^2)^{3/2}}. \quad (2)$$

For a given reduced volume the sequence of shapes for several Δa values was calculated. The characteristic dimensions of the axisymmetrical shape, the height (L_h), which is the maximal diameter, and the width (L_w), which is the maximal projection along symmetry axis (Fig. 4b), were determined. These two dimensions correspond to the sides of the minimal rectangle into which the vesicle shape fits. The ratio between the height and the width of the vesicle ($P_1 = L_w/L_h$) is unique for a given volume and is a monotonic function of Δa (Fig. 5).

The described characteristic dimensions, especially the width (L_w), can only be measured if the rotational symmetry axis of an observed vesicle is perpendicular to the optical axis of the microscope. Because vesicles float freely in the solution, this is not always the case. For vesicles where L_w cannot be measured, the shape and consequent Δa values are determined from the ratio between the L_h and twice the radius of the outer sphere of the limiting shape ($P_2 = L_h/(2R_L)$) (Fig. 4a).

The experimental sequence is obtained by recording the vesicle contour over a period of time, for which the shapes

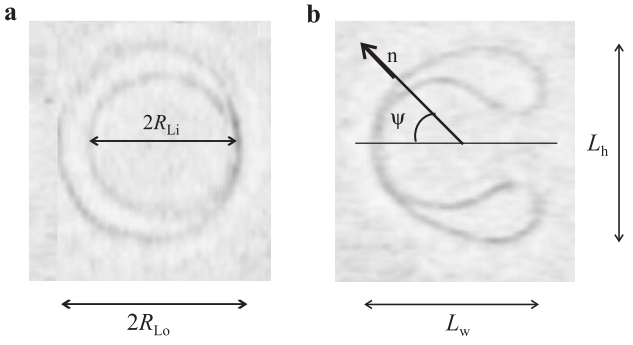

Fig. 4. Images of the vesicle shapes with indicated parameters which are used for determining of the reduced volume and the reduced area difference: (a) R_{Lo} and R_{Li}, which are the radii of the limiting shape, (b) height (L_h), which is the maximal diameter of the vesicle shape, and width (L_w), which is the maximal projection of the vesicle shape along a symmetry axis, are taken as characteristic dimensions of the axisymmetrical shape of a vesicle. ψ is the angle between the normal to the contour and the symmetry axis of the vesicle.

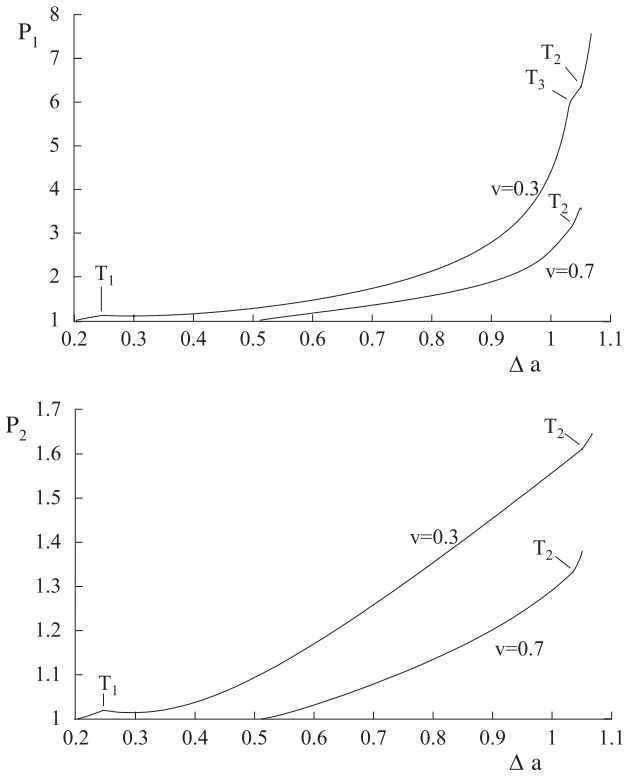

Fig. 5. Dependence of ratios $P_1 = L_h/L_w$ and $P_2 = L_h/2R_L$ on reduced area difference (Δa) for two reduced volumes: 0.3 and 0.7. T_1 denotes the points where parts of the membranes detach from each other, T_2 denotes the points where the shape changes from the mirror symmetric to non-mirror symmetric shape, and point T_3 denotes the change in determination of the width (L_w), i.e., the point where the widest part of the shape moves to the symmetrical axis of the vesicle.

were calculated as a function of Δa_0. Because we usually analyze only a small part of the observed sequence such that the changes of Δa_0 are relatively small, a linear approximation can be assumed for the decrease of Δa_0 with time:

$$\Delta a_0 = -\gamma(t - t_0), \tag{3}$$

where t_0 indicates the time at which the outer and the inner membrane leaflets have the same equilibrium area, and the parameter γ measures the rate of the decrease of Δa_0. The parameters γ and t_0, together with the reduced volume and the ratio k_r/k_c, are determined by minimizing the sum of normalized squares: $\Sigma_1 = \Sigma_i((P_{1i}^{exp} - P_{1i})/P_{1i}^{exp})^2$ or $\Sigma_2 = \Sigma_i ((P_{2i}^{exp} - P_{2i})/P_{2i}^{exp})^2$, where P_{1i}^{exp} and P_{2i}^{exp} are measured ratios and P_{1i} and P_{2i} are corresponding calculated values.

3. Results

The last stage of typically observed vesicle shape transformations (Fig. 1) is the transformation from an oblate discocyte to the stomatocyte with closed neck. Observed sequences of shape transformations matched well with those calculated for decreasing Δa_0 (Fig. 6). At small reduced volumes ($v < 0.4$), the theory predicts that the area of the

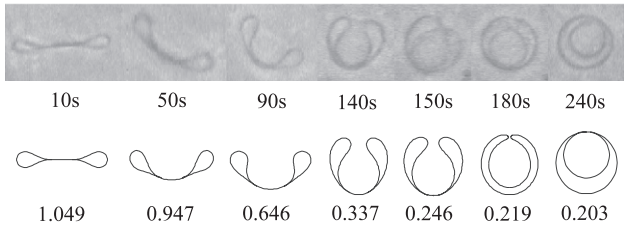

Fig. 6. Some shapes of a vesicle, taken at given times, and theoretical shapes for different reduced equilibrium area differences of the two membrane monolayers (Δa_0) for the reduced volume 0.32, and the ratio between the nonlocal bending modulus and the bending modulus, k_r/k_c, of 3. It should be noted that the area of the membrane in contact appears to be much larger than it actually is, because of the finite thickness of the line.

double bilayer section of the vesicle vanishes before the closing of the neck (Fig. 6, the theoretical shape for $\Delta a_0 = 0.219$). Observations show that the area of the double bilayer does diminish, but some parts of the membrane appear to remain in contact right up to the closing of the neck. The observed narrowing of the neck is continuous for all the vesicles analyzed, regardless of their real size (R_0). The time taken for the neck to close can be only approximately estimated, because the small neck can be observed only if the rotational symmetry axis of the vesicle is strictly perpendicular to the optical axis of the microscope, which it was not most of the time.

Our results, including the values of the parameters obtained from the best fits, the reduced volumes determined from the limiting shapes (v_L), and the experimentally estimated time (t_L) of the closing of the neck, are listed in Table 1 for 10 vesicles with reduced volumes between 0.24 and 0.64.

In Fig. 7 the measured ratios, P_1 and P_2, and the best fit are shown as a function of time for the two vesicles (nos. 1 and 9 in Table 1). To check the procedure, we compared the values for the reduced volume (v) obtained from the fitting

Table 1
Results for 10 shape sequences, and the comparison of values obtained from the fits and directly from the observed shapes

i	Type	k_r/k_c	v	t_{clo} (s)	γ ($\times 10^{-3}$ s^{-1})	v_L	t_L (s)
1	P1, cont.	2.4	0.32	234	6.08	0.33	306
2	P2, cont.	2.6	0.45	149	5.18	0.44	112
3	P2, cont.	8.1	0.24	378	4.19	0.32	316
4	P1, discont.	3.8	0.60	529	2.01	0.67	466
5	P2, cont.	0.7	0.34	59	20.58	0.41	79
6	P1, discont.	1.6	0.47	901	1.15		
7	P2, cont.	3.0	0.29	781	1.61	0.38	564
8	P2, cont.	1.4	0.31	764	1.62	0.4	668
9	P2, discont.	4.3	0.64	536	1.28	0.68	365
10	P2, cont.	1.8	0.33	191	7.53	0.38	331

Column Type indicates which of the ratios P_1 and P_2 and which type of the transition (continuous or discontinuous) was used for the fitting procedure. k_r/k_c is the ratio between the nonlocal and the local bending constant; v, t_{clo} and γ are the reduced volume, the time of the closing of the neck and the rate of decrease of Δa_0, respectively, determined from the fit. v_L and t_L are the corresponding volume and time of closing of the neck obtained directly from the observed time sequence of the shapes.

procedure with the volume (v_L) determined from the limiting shape, and the predicted times of closing of the neck (t_{clo}) with the observed ones (t_L) listed in Table 1. To determine how accurately the ratio k_r/k_c can be assessed by the described method, the best fit for the reduced volume (v) and the parameters γ and t_0 was performed for several ratios k_r/k_c, and the sum of normalized least squares was calculated. The dependence of these sums on the ratio k_r/k_c is presented in Fig. 8. Determination of the ratio k_r/k_c was quite accurate if the vesicle was in the appropriate orientation during the measurements so that we could use the ratio P_1 (Fig. 8A). The reliability of k_r/k_c determination is less if the ratio P_2 had to be used (Fig. 8B).

The ratio k_r/k_c should be the same for all vesicles, since they are prepared from the same lipid. If we compare the results for 10 vesicles (Table 1) and take into consideration the experimental error, it can be stated confidently that for SOPC the value of the ratio k_r/k_c is between 1.5 and 3.5. The problem in obtaining an accurate fit can partly be ascribed to thermal fluctuations of the vesicle shape. The observed average shape of the fluctuating vesicle in general differs from the equilibrium one [25]. However, constraints of constant membrane area and vesicle volume are important for prolate shapes [25], but not so critical for the stomatocyte and codocyte shapes, where the most pronounced fluctuation mode is "opening and closing of the neck".

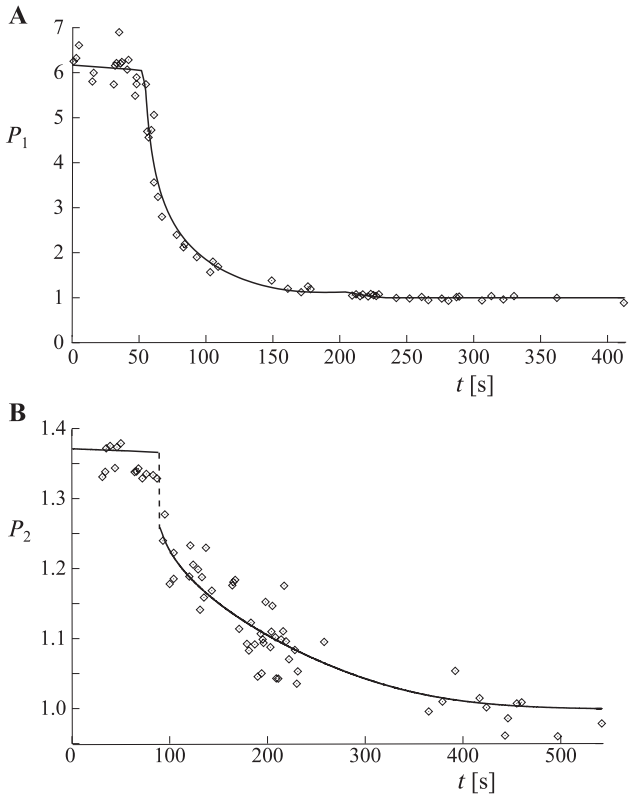

Fig. 7. The measured values of ratios P_1 (A) and P_2 (B) for vesicle nos. 1 and 9, respectively, as function of time. The lines are the best fits of calculated ratios for $k_r/k_c = 2.5$ and $k_r/k_c = 4.3$ and reduced volumes $v = 0.32$ and $v = 0.64$, respectively.

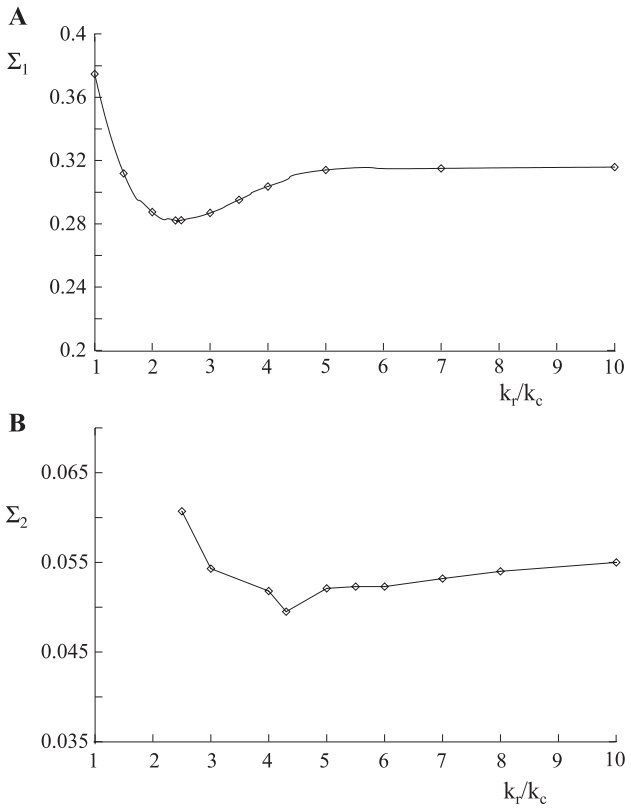

Fig. 8. The accuracy of the determination of the ratio k_r/k_c. For each value of the ratio k_r/k_c, the best fit on measured values of ratios P_1 and P_2 for the reduced volume (v) and the parameters K and t_0 was obtained, and the sum of normalized least squares was calculated, $\Sigma_1 = \Sigma_i((P_{1i}^{exp} - P_{1i})/P_{1i}^{exp})^2$ and $\Sigma_2 = \Sigma_i((P_{2i}^{exp} - P_{2i})/P_{2i}^{exp})^2$, for the vesicles with reduced volumes 0.32 (A) and 0.64 (B), respectively.

Thus, we believe that the stomatocyte and codocyte vesicles fluctuate around the shape, which is close to the calculated equilibrium shape.

We also observed shape transitions on some vesicles with larger reduced volumes. Such vesicles are nearly spherical so that the ratios P_1 and P_2 are close to 1.0 over the entire period of observation. Therefore, and because of shape fluctuations, these ratios could not be precisely determined and such vesicles were not further analyzed. Nevertheless, it is interesting that the transition from a nearly spherical shape to the sphere with invagination with closed neck was observed to take place almost instantly.

4. Discussion

In this section, we shall first review the model of membrane elasticity used and the corresponding theoretical analysis of the shapes and then we shall discuss the method of analysis and the reliability of the results.

It is widely accepted that vesicle shapes can be well described by the ADE model [6,16,26]. In addition to the bending of the membrane, this model also takes into consideration the nonlocal bending. The shape of a vesicle

is determined by the reduced volume, by the ratio k_r/k_c, the reduced equilibrium area difference and the spontaneous curvature. During our experiments, the reduced volume (v) of a given vesicle and the ratio k_r/k_c remained constant. Also it can be taken that the spontaneous curvature of bilayer membrane is zero, since the membrane is symmetrical. The vesicles were prepared from SOPC only and the same solution is on the both sides of the membrane.

The vesicle shapes for which parts of membrane are in contact, i.e., torocytes and codocytes, were previously analyzed theoretically in an approximate manner by Deuling and Helfrich [24]. In our analysis of torocyte and codocyte shapes (Appendix A), the curvature of the membrane at the rim of double bilayer is considered to be continuous, because there is no external torque acting (cp. Eq. (A16)). Moreover, the contours of the section of torocytes and codocytes, where the bilayers are not in contact, are calculated by considering the longitudinal force (F_2) in the differential equation (Eq. (A11)) (cp. Ref. [27]). It is also taken into consideration that curvatures of codocytes can vary over the area of the double bilayer section.

For the vesicles with reduced volume around 0.7 and the ratio $k_r/k_c = 3$, theory predicts a discontinuous shape change from discocyte to almost closed stomatocyte (Fig. 3). However, such sudden jumps of the vesicle shape were not observed. This could mean that the ratio k_r/k_c is larger than 6, i.e., the value above which the predicted transitions are continuous for this volume. However, an alternative possibility was that instantaneous large changes in vesicle shape can also not occur because due to the rearrangement of the surrounding viscous aqueous medium large shape changes take some time. Thus, the experimentally obtained shape transition is necessarily continuous. It is almost impossible to distinguish between these two possibilities. But we observed that for some nearly spherical vesicles (which we did not analyze and are not included in the Table 1), where relatively less solution has to be moved, the transition from starting an invagination, visible as enhanced fluctuations, to closing of the neck occurs very fast. We reason that measurements are more reliable if done on vesicles with lower volumes, where a continuous transition is predicted.

For lower vesicle volumes, where some parts of the membrane are in contact, we assume that there is no interaction between the bilayers in the double bilayer vesicle section. The model predicts a continuous transition from codocyte to a stomatocyte shape characterized by an open neck, followed by a continuous closing of the neck (Fig. 3). The observed closing of the neck is continuous; however, stomatocyte shapes with an open neck (Fig. 6) were not detected. One possible reason could be that some attraction exists between the bilayers in double bilayer, which decreases the energy of a vesicle [28]. Theoretically this could be approximately accounted for by adding to Eq. (1) an energy term: $-Wa_s$, where a_s is the area of the double bilayer and the parameter W is the adhesion constant expressed relative to the bending elastic constant ($W = 2wR_0^2/k_c$, where w is the adhesion constant) [29]. Such attraction stabilizes the codocyte shapes (region IV in Fig. 2) over a larger part of the phase diagram. Therefore, the adhesion between the membrane bilayers could explain the persistence of the membrane contact up to attaining the limiting shape. However, the adhesion term disfavors shapes with narrow necks and predicts a discontinuous closing of the neck (Božič, unpublished results). We assume that the adhesion constant (w) should be the same for different vesicles, because of the same membrane composition and the same solution in the vesicles. The bending energies do not depend on vesicle size, so the influence of adhesion on the vesicle shape would be more pronounced for larger vesicles. Regardless of the vesicle size, no discontinuous closing of the neck was observed and the observed shape sequences for comparable reduced volumes were similar. So we can conclude that neglecting the interaction between the membranes in the double bilayer was reasonable.

The observations are consistent with the notion that Δa_0 decreases during the observation. Possible reasons for this decrease could be the flip-flop of the molecules from the outer to the inner membrane leaflet, a decrease in the number of molecules in the outer, or an increase in the number of molecules in the inner leaflet. Spontaneous net flow of phospholipid molecules from one leaflet to the other is a relaxation process, driven by the lowering of the vesicle elastic energy. This process ends when the vesicle attains the shape with the minimum bending energy corresponding to its volume. This is a prolate ellipsoid for large reduced volumes, a discocyte shape for reduced volumes around 0.6, and a nearly closed stomatocyte shape for lower reduced volumes [30]. Our observations show that the transitions of vesicle shapes to stomatocyte shapes with closed necks occur also with vesicles with reduced volumes larger than 0.6, which indicates that there is an additional mechanism to decrease Δa_0. It is reasoned that vesicles should not be considered as isolated systems, but that phospholipid molecules may exchange between the outside membrane monolayers and the surrounding solution. The critical vesicle concentration (CVC) [22] is very low (10^{-10} M), but in our case it should be taken in consideration. In our preparation, we mixed equal parts (0.2 ml) of vesicle solution and isomolar solution without vesicles just before the observation. A possible way to restore the equilibrium CVC is for some molecules from the outside membrane monolayer to leave the membrane. In our case this means 1.2×10^{10} molecules, which is enough to change the shape from discocyte to sphere with an invaginated smaller sphere for 8000 vesicles with radii 5 μm. Our estimate is that the average sample contained considerably less than 8000 vesicles. Moreover, the presence of hydrophobic surfaces (like the surface between water and grease, used as a spacer in the observation chamber) can increase the number of phospholipid molecules which leave the membrane, because

some molecules from the solution may assemble on such surfaces.

Although the exact reason or the combinations of reasons for the decreasing Δa_0 cannot be determined from our experiments, we estimate that a linear approximation (Eq.(3)) can be used, because the analyzed sequence takes just a small part (1/10) of the duration of the entire shape sequence (Fig. 1). Also, after closing the neck of an observed vesicle, the process of dissolution is not finished, because other vesicles can be found in the same observation chamber, which are still going through the process of shape transformations.

The inclusion of the nonlocal bending energy term is crucial to describing the observed vesicle shape changes due to decreasing equilibrium area difference. For the shape transformation of a vesicle in proper orientation, the ratio k_r/k_c can be determined quite well. However, the order of magnitude for the ratio k_r/k_c can be determined irrespective of the vesicle volume or its orientation. If we critically evaluate the results for 10 vesicles, the value $k_r/k_c = 2.5 \pm 1$ is obtained.

Appendix A. Differential equation and boundary conditions

In this Appendix, we present a rigorous derivation of the differential equation for the membrane shape and of the boundary conditions of stomatocytic and codocytic vesicles. The equilibrium shapes are obtained by minimizing the elastic energy at given conditions, where the interaction energy between bilayers is neglected. All dimensions of the vesicle shapes are given relative to the radius $R_0=(A/4\pi)^{1/2}$ of the sphere with the same area A.

The equilibrium states of the stomatocyte are the extremes of the elastic energy defined in Eq. (1) at given vesicle volume and membrane area. Because we consider the stomatocytes that have fixed volume and area, the extremes of the elastic energy correspond to the stationary points of the functional

$$g = w_b + w_r - M(v - v_0) + L(a - 1), \tag{A1}$$

where the reduced volume ($v = 3V/4\pi R_0^3$) and the reduced membrane area ($a = A/(4\pi R_0^2) = 1$) are fixed. The constraints in reduced volume and reduced area are incorporated in the energy minimization by introducing the Lagrange multipliers $M = R_0^3\Delta p/6k_c$ and $L = R_0^2\lambda/2k_c$, where Δp is the difference between the pressure in the vesicle and the pressure in the vesicle surroundings, and λ is the lateral tension.

In the stationary point, the variation of the functional (Eq. (A1)) with respect to arbitrary shape deviation is zero. Written out, the variation of g is

$$\delta g = \delta w_b + N\delta\Delta a - M\delta v + L\delta a, \tag{A2}$$

where the parameter N represents the difference between the lateral tensions of the outer and inner monolayers and is expressed in terms of the area difference Δa_0 through the equation

$$N = 2\frac{k_r}{k_c}(\Delta a - \Delta a_0). \tag{A3}$$

The observed vesicles are axisymmetric, therefore we can parameterize the vesicle shape in terms of its axisymmetric contour and express the functional in terms of an integral over this contour. An axisymmetric surface can be parameterized by the angle between the normal to the contour and the symmetry axis of the shape ($\psi(s)$) (Fig. 4), where s is the arc length along the contour. The coordinates $r(s)$ and $z(s)$, which represent the distance between the symmetry axis and a point on the contour of the vesicle membrane and the position along the symmetry axis, respectively, depend on ψ(s) through

$$\dot{r} = \cos\psi, \quad \dot{z} = \sin\psi, \tag{A4}$$

where the dot denotes the derivation with respect to the arc length (s). Three points on the contour should be mentioned; point A is the starting point, which lies at the pole of the vesicle, and points B and C are at the rim of the double bilayer, but at different arc lengths (s). Using integral expressions for the reduced volume, the reduced area and the reduced difference between the monolayer areas,

$$v = \frac{3}{4}\int_B^C r^2\sin\psi ds, \tag{A5}$$

$$a = \int_A^B rds + \int_B^C rds \tag{A6}$$

and

$$\Delta a = \frac{1}{4}\int_B^C r\left(\frac{\sin\psi}{r} + \dot{\psi}\right)ds, \tag{A7}$$

we can express the variation of the functional g as

$$\delta g = \delta\int_A^B \ell_1 ds + \delta\int_B^C \ell_2 ds, \tag{A8}$$

where Lagrangian functions for both parts ℓ_i ($i = 1, 2$) can be written as:

$$\begin{aligned}\ell_i = {} & \frac{(3-i)r}{8}\left(\frac{\sin\psi}{r} + \dot{\psi}\right)^2 + (i-1)N\frac{\sin\psi + \dot{\psi}r}{4} \\ & - (i-1)M\frac{3r^2\sin\psi}{4} + (3-i)L\frac{r}{2} + \Gamma(\dot{r} - \cos\psi) \\ & + F(\dot{z} - \sin\psi).\end{aligned} \tag{A9}$$

The additional Lagrange multipliers $\Gamma(s)$ and $F(s)$ have to be introduced because the variables $r(s)$, $z(s)$ and $\psi(s)$ are not independent but are related through Eq. (A4). The index

i is 1 when referring to the vesicle double bilayer section, where parts of the membrane are in contact, and is 2 when referring to the other section of the vesicle. The factor $(3-i)$ in Eq. (A9) indicates that the bending energy and the lateral tension of the double bilayer are twice the bending energy and the lateral tension of the bilayer. While the double bilayer is composed of the two oppositely oriented bilayers belonging to the same membrane, the relative tension of one bilayer compensates the relative tension of the other and the pressure is the same at both sides of the double bilayer.

The variation of the functional with respect to shape is zero ($\delta g=0$) if the Euler–Lagrange equations and the boundary conditions are fulfilled. By performing the variation and eliminating Γ and s from the Euler–Lagrange equations [27,31] of both sections, we obtain the differential equation for the double bilayer,

$$\frac{r}{2\cos^2\psi}\left(\frac{\sin\psi}{r}\left(\frac{\sin^2\psi}{r^2}-\cos^2\psi\psi'^{\,2}\right)-4L\frac{\sin\psi}{r}+4F_1\frac{1}{r^2}\right)-\frac{\cos\psi\psi'}{r}+\frac{\sin\psi}{r^2}-\cos\psi\psi''+\sin\psi\psi'^{\,2}=0 \qquad \text{(A10)}$$

and the differential equation for the rest of the vesicle,

$$\frac{r}{2\cos^2\psi}\left(\frac{\sin\psi}{r}\left(\frac{\sin^2\psi}{r^2}-\cos^2\psi\psi'^{\,2}\right)-6M+4L\frac{\sin\psi}{r}+2N\frac{\sin^2\psi}{r^2}-8F_2\frac{1}{r^2}\right)-\frac{\cos\psi\psi'}{r}+\frac{\sin\psi}{r^2}-\cos\psi\psi''+\sin\psi\psi'^{\,2}=0, \qquad \text{(A11)}$$

where the prime denotes the derivative with respect to the coordinate (r). The Euler–Langrange equations show that F_1 and F_2 are constant.

The minimization procedure also gives the boundary conditions that are described by the equation

$$\left[\frac{\partial\ell_1}{\partial\dot r}\delta r+\frac{\partial\ell_1}{\partial\dot\psi}\delta\psi+\frac{\partial\ell_1}{\partial\dot z}\delta z+\frac{\partial\ell_1}{\partial\dot\Gamma}\delta\Gamma+\frac{\partial\ell_1}{\partial\dot F}\delta F-H_1\delta s\right]_{\mathrm{A}}^{\mathrm{B}}+\left[\frac{\partial\ell_2}{\partial\dot r}\delta r+\frac{\partial\ell_2}{\partial\dot\psi}\delta\psi+\frac{\partial\ell_2}{\partial\dot z}\delta z+\frac{\partial\ell_2}{\partial\dot\Gamma}\delta\Gamma+\frac{\partial\ell_2}{\partial\dot F}\delta F-H_2\partial s\right]_{\mathrm{B}}^{\mathrm{C}}=0, \qquad \text{(A12)}$$

where

$$H_i=\frac{(3-i)r}{8}\left(\dot\psi^2-\frac{\sin^2\psi}{r^2}\right)+\frac{(i-1)N\,\sin\psi}{4}+\frac{3(i-1)Mr^2\sin\psi}{4}+\frac{(3-i)Lr}{2}+\Gamma\cos\psi+F_i\sin\psi \qquad \text{(A13)}$$

are the Hamiltonian functions for the double bilayer ($i=1$), and for the rest of the vesicle ($i=2$). The Hamiltonian functions are constant because the Lagrange functions (Eq. (A9)) do not depend on s. Moreover, the Hamiltonian functions equal zero, due to arbitrary lengths of both sections and consequently arbitrary δs at the contour ends. The multiplicator F_1 also equals zero, because the length of the double bilayer along the symmetry axis is arbitrary ($\delta z|_{\mathrm{B}}-\delta z|_{\mathrm{A}}\neq 0$). By using $\frac{\partial\ell_1}{\partial\dot\psi}\delta\psi\Big|_{\mathrm{A}}=\frac{r\dot\psi+\sin\psi}{2}\delta\psi\Big|_{\mathrm{A}}=0$. it can be shown that the surfaces are smooth at the poles of the vesicle because the variation of $\delta\psi$ in the point A is arbitrary. The boundary conditions at junction points B and C are interrelated because of the same radius and the coordinate z and the fixed difference between the angles at these points ($\psi_{\mathrm{C}}=\psi_{\mathrm{B}}+\pi$).

Written out, the condition $\frac{\partial\ell_1}{\partial\dot\psi}\delta\psi\Big|_{\mathrm{A}}^{\mathrm{B}}+\frac{\partial\ell_2}{\partial\dot\psi}\delta\psi\Big|_{\mathrm{B}}^{\mathrm{C}}=0$ leads to

$$c_m\,|_{\mathrm{B}-}=\frac{c_{\mathrm{m}}\,|_{\mathrm{B}+}-c_{\mathrm{m}}\,|_{\mathrm{C}-}}{2}, \qquad \text{(A14)}$$

where $c_{\mathrm{m}}|_{\mathrm{B}-}$, $c_{\mathrm{m}}|_{\mathrm{B}+}$, $c_{\mathrm{m}}|_{\mathrm{C}-}$ are curvatures along the meridians at the rim of the double bilayer section and at the two rims of the other section of the vesicle, respectively. The condition $\frac{\partial\ell_1}{\partial\dot r}\delta r\Big|_{\mathrm{A}}^{\mathrm{B}}+\frac{\partial\ell_2}{\partial\dot r}\delta r\Big|_{\mathrm{B}}^{\mathrm{C}}=0$ leads to

$$\Gamma\,|_{\mathrm{B}-}=\Gamma\,|_{\mathrm{B}+}-\Gamma\,|_{\mathrm{C}-}, \qquad \text{(A15)}$$

where $\Gamma|_{\mathrm{B}-}$, $\Gamma|_{\mathrm{B}+}$, $\Gamma|_{\mathrm{C}-}$ are transfer shear forces in a radial direction at the same places. Because the coordinate z in point B equals the coordinate z in point C, the condition $\frac{\partial\ell_2}{\partial\dot z}\delta z\Big|_{\mathrm{B}}^{\mathrm{C}}=0$ is automatically fulfilled, therefore the parameter F_2 need not to be zero. We can also show that the curvature at the point C is opposite to the curvature at point B by writing out the expression $H_2|_{\mathrm{B}+}+H_2|_{\mathrm{C}-}-H_1|_{\mathrm{B}}=0$. By also considering Eqs. (A14) and (A15), we obtain

$$c_{\mathrm{m}}\,|_{\mathrm{B}+}=c_{\mathrm{m}}\,|_{\mathrm{B}-}. \qquad \text{(A16)}$$

The first boundary condition (Eq. (A15)) shows that the transfer shear force is conserved at the junction of the sections, so there is no net force at the junction (line) point. Because there is no external torque, the curvature along the meridians should be the same at the junction of the sections, which is described by the second boundary condition (Eq. (A16)).

References

[1] H. Hotani, Transformation pathways of liposomes, J. Mol. Biol. 178 (1984) 113–120.

[2] J. Kaes, E. Sackmann, Shape transitions and shape stability of giant phospholipid-vesicles in pure water induced by area-to-volume changes, Biophys. J. 60 (1991) 825–844.

[3] W. Wintz, H.-G. Döbereiner, U. Seifert, Starfish vesicles, Europhys. Lett. 33 (1996) 403–408.

[4] S. Svetina, M. Brumen, B. Žekš, Lipid bilayer elasticity and the bilayer couple interpretation of red cell shape transformations and lysis, Stud. Biophys. 110 (1985) 177–184.

[5] B. Božič, S. Svetina, B. Žekš, R.E. Waugh, Role of lamellar mem-

brane-structure in tether formation from bilayer vesicles, Biophys. J. 61 (1992) 963–973.
[6] L. Miao, U. Seifert, M. Wortis, H.-G. Döbereiner, Budding transitions of fluid-bilayer vesicles—the effect of area-difference elasticity, Phys. Rev., E 49 (1994) 5389–5407.
[7] W. Rawicz, K.C. Olbrich, T. McIntosh, D. Needham, E. Evans, Water permeability and mechanical strength of polyunsaturated lipid bilayers, Biophys. J. 79 (2000) 328–339.
[8] L. Fernandez-Puente, I. Bivas, M.D. Mitov, P. Meleard, Temperature and chain-length effects on bending elasticity of phosphatidylcholine bilayers, Europhys. Lett. 28 (1994) 181–186.
[9] H.P. Duwe, J. Kaes, E. Sackmann, Bending elastic-moduli of lipid bilayers-modulation by solutes, J. Phys. (France) 51 (1990) 945–962.
[10] J.F. Faucon, M. Mitov, P. Meleard, I. Bivas, P. Bothorel, Bending elasticity and thermal fluctuations of lipid-membranes—theoretical and experimental requirements, J. Phys. (France) 50 (1989) 2389–4214.
[11] M.B. Schneider, J.T. Jenkins, W.W. Webb, Thermal fluctuations of large cylindrical phospholipid-vesicles, Biophys. J. 45 (1984) 891–898.
[12] G.R. Beblik, R.M. Servuss, W. Helfrich, Bilayer bending rigidity of some synthetic lecithins, J. Phys. (Paris) 10 (1985) 1773–1778.
[13] R.E. Waugh, J. Song, S. Svetina, B. Žekš, Local and nonlocal curvature elasticity in bilayer-membranes by tether formation from lecithin vesicles, Biophys. J. 61 (1992) 974–982.
[14] R.M. Raphael, R.E. Waugh, Accelerated interleaflet transport of phosphatidylcholine molecules in membranes under deformation, Biophys. J. 71 (1996) 1374–1388.
[15] S. Svetina, B. Žekš, R.E. Waugh, R.M. Raphael, Theoretical analysis of the effect of the transbilayer movement of phospholipid molecules on the dynamic behavior of a microtube pulled out of an aspirated vesicle, Eur. Biophys. J. 27 (1998) 197–207.
[16] H.-G. Döbereiner, E. Evans, M. Kraus, U. Seifert, M. Wortis, Mapping vesicle shapes into the phase diagram: A comparison of experiment and theory, Phys. Rev., E 55 (1997) 4458–4474.
[17] H.-G. Döbereiner, G. Gompper, C.K. Haluska, D.M. Kroll, P.G. Petrov, K.A. Riske, Advanced flicker spectroscopy of fluid membranes, Phys. Rev. Lett. 91 (4) (2003) 048301.
[18] R. Bar-Ziv, E. Moses, P. Nelson, Dynamic excitations in membranes induced by optical tweezers, Biophys. J. 75 (1998) 294–320.
[19] S. Svetina, B. Žekš, Membrane bending energy and shape determination of phospholipid-vesicles and red blood-cells, Eur. Biophys. J. 17 (1989) 101–111.
[20] U. Seifert, K. Berndl, R. Lipowsky, Shape transformations of vesicles-phase-diagram for spontaneous-curvature and bilayer-coupling models, Phys. Rev., A 44 (1991) 1182–1202.
[21] J.P. Reeves, R.M. Dowben, Formation and properties of thin-walled phospholipid vesicles, J. Cell. Physiol. (1973) 49–60.
[22] D.D. Lasic, Liposomes: From Physics to Applications, Elsevier, Amsterdam, 1993.
[23] E.A. Evans, Minimum energy analysis of membrane deformation applied to pipet aspiration and surface-adhesion of red-blood-cells, Biophys. J. 30 (1980) 265–284.
[24] H.J. Deuling, W. Helfrich, The curvature elasticity of fluid membranes: a catalogue of vesicles shapes, J. Phys. (Paris) 37 (1976) 1335–1345.
[25] V. Heinrich, F. Sevšek, S. Svetina, B. Žekš, Large deviations of the average shapes of vesicles from equilibrium: Effects of thermal fluctuations in the presence of constraints, Phys. Rev., E 55 (1997) 1809–1818.
[26] V. Heinrich, S. Svetina, B. Žekš, Nonaxisymmetric vesicle shapes in a generalized bilayer-couple model and the transition between oblate and prolate axisymmetrical shapes, Phys. Rev., E 48 (1993) 3112–3123.
[27] F. Jülicher, U. Seifert, Shape equations for axisymmetrical vesicles—a clarification, Phys. Rev., E 49 (1994) 4728–4731.
[28] R. Lipowsky, Generic interactions of flexible membranes, in: R. Lipowsky, E. Sackmann (Ed.), Handbook of Biological Physics, Structure and Dynamics of Membranes, vol. 1, Elsevier, Amsterdam, 1995, pp. 521–603.
[29] U. Seifert, R. Lipowski, Adhesion of vesicles, Phys. Rev., A 42 (1990) 4768–4771.
[30] S. Svetina, B. Božič, J. Majhenc, B. Žekš, Mechanical properties of closed lamellar membranes and cellular processes, Nonlinear Anal.-Theor. 47 (2001) 269–280.
[31] B. Božič, S. Svetina, B. Žekš, Theoretical analysis of the formation of membrane microtubes on axially strained vesicles, Phys. Rev., E 55 (1997) 5834–5842.